Proceedings of 2021 IEEE
International Conference on Mechatronics and Automation
August 8 - 11, Takamatsu, Japan

A Combined Indoor Self-positioning Method for Robotic Fish Based on Multi-sensor Fusion

Yuzhuo Fu[1,2], Ben Lu[1,2], Xiaocun Liao[1,2], Qianqian Zou[1,2], Zhuoliang Zhang[1,2] and Chao Zhou[1]

[1]*State Key Laboratory of Management and Control for Complex Systems, Institute of Automation, CAS, Beijing 100190, China*
[2]*School of Artificial Intelligence, University of Chinese Academy of Sciences, Beijing 100049, China*

{*fuyuzhuo2019, luben2019, liaoxiaocun2019, zouqianqian2019, zhangzhuoliang2018@ia.ac.cn, chao.zhou*}@ia.ac.cn

2021 IEEE International Conference on Mechatronics and Automation (ICMA) | 978-1-6654-4101-8/21/$31.00 ©2021 IEEE | DOI: 10.1109/ICMA52036.2021.9512608

Abstract **- In an experimental environment with limited conditions, it is always hard to achieve precise positioning of robotic fish. A combined indoor self-positioning method in this paper is introduced to solve the problem. For the short-distance range, coordinates are calculated by fusing the measured distances and angles. For the medium-distance range, a clustering-grid supervision (CGS) algorithm is proposed and adopted to correct the coordinates obtained by the four-point positioning method. An ostracion-like robotic fish is used as the experimental object to achieve centimeter-level positioning with an average positioning error of 4.492 cm in a short-distance range and decimeter-level positioning with an error of 2.049 dm in a medium-distance range. Compared with traditional methods, this comprehensive method has the advantages of low cost and high accuracy.**

Index Terms **- multi-sensor fusion, robotic fish, indoor positioning**

I. Introduction

Robotics involves a number of top technology fields, including positioning, navigation, control, and sensor technology. Among them, the research on robot positioning method has been started since the 1960s [1]. Autonomous positioning technology is the core technology of mobile robots. Accurate and stable positioning is an important prerequisite for robots to achieve more functions and tasks.

As a combination of fish propulsion mechanism and robotic technology, robotic fish provides a new idea for the development of new underwater vehicles, and has important research value and application prospects. MIT invented the first real tuna-like robotic fish Robotuna [2], and since then started the study of bionic robotic fish. In recent years, researches on robotic fish have also emerged one after another. Li et al. developed an electronic fish driven only by a soft electroactive structure made of dielectric elastomer and ion-conducting hydrogel [3]. And the Tunabot developed by Zhu et al. has a swimming speed of 4 BL/s, and the difference in the tail flow field at different frequencies was quantitatively analyzed [4]. Muralidharan et al. used shape-memory alloys to design a sub-trout robotic fish, which can restore the true fish swimming posture to the greatest extent [5].

The motion characteristics of robotic fish and the particularity of the underwater environment make the robotic fish positioning problem more challenging than traditional indoor positioning. Wang et al. used cameras and inertial measurement units, combined with Monte Carlo positioning, to achieve limited-range positioning of micro underwater robots [6]; Novak et al. deployed sound sources in the robotic fish and its water tank and designed based on the spectrum ratio of the two The positioning algorithm realizes the spatial positioning of the robotic fish [7]; Zheng et al. use a pressure sensor to construct a lateral line perception system, and use the acquired flow field information to calculate the robotic fish motion trajectory [8].

The current robotic fish positioning in the experimental environment has the following difficulties in realization: 1) The performance of the sensor used in the traditional method may change or even fail completely in the water. 2) The robotic fish usually presents a regular motion like bowing during its swimming process. This regular motion will interfere with the data sampling and sensor layout in the robot fish positioning. 3) Considering the size of experimental pool and sensors for the indoor robotic fish positioning, those methods based on GPS, INS, DVL, etc. cannot be basically used.

All in all, the combined positioning system implemented in this article provides corresponding positioning solutions for different distance ranges. Using infrared sensor, IMU, monocular camera, BLE base station and its signal receiving node and other sensor equipment, combined with the clustering-grid supervision algorithm proposed in this paper, centimeter-level and decimeter-level robotic fish positioning in short and medium range are respectively achieved. The positioning scheme based on multi-sensor fusion is suitable for real-time tracking and motion performance analysis, providing a new idea for indoor robotic fish positioning research.

II. Mechanical Structure and Sensor Layout

The positioning method implemented in this paper uses a ostracion-like robotic fish as the experimental object, and the fish body structure is shown in Fig. 1. The fish body is a rectangular parallelepiped as a whole, and the fish tail uses a single steering gear to drive the robotic fish. This robotic fish is made of nylon material.

As shown in Fig. 1, the inside of the fish body includes a main control circuit board equipped with STM32F4, which controls the sensors and steering gear; three infrared distance sensors are equipped on both sides and front of the fish to measure the distance between the fish and each pond wall. A camera equipped on the head of the fish body is used for taking images of the front of the fish. The fish is equipped with two IMUs to obtain the angle information. All the above sensors are used for short range positioning; the top of the fish is equipped with a BLE beacon. It is used to coordinate with 4 signal receiving nodes to locate fish in the medium-distance range.

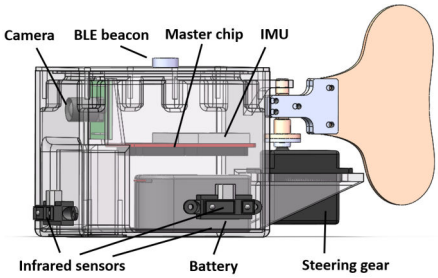

Fig. 1 Mechanical structure and sensor arrangement

III. Positioning Method

This part will introduce the positioning principle in short-distance range and medium-distance range respectively.

A. Short-distance positioning

For a short distance range (within about 1 meter), the camera is used to capture the image of front of the robotic fish to determine the initial orientation, and then combines multiple infrared sensors and IMU to calculate the specific trajectory of the robotic fish during its swimming process. Thus, the positioning of the robotic fish with an error of centimeter level is completed.

1) Initial orientation determination

Signs of different colors are pasted on the four walls of the experimental water pond, and the camera at the front of the fish body captures different color blocks to distinguish the initial orientation of the robotic fish[9]. The specific steps are shown in Fig. 2. The initial direction is determined by extracting the HSV value of the detected color block.

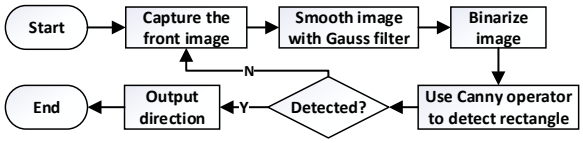

Fig.2 Flowchart of image processing

2) Coordinate calculation of robotic fish

In the experiment, the measured distance value cannot be directly used as its coordinate. It is necessary to combine the measured distance value with the current angle and orientation of the fish. The yaw angle of the robotic fish in this subject changes greatly during the movement, the pitch angle remains unchanged and the roll angle is so small that can be ignored.

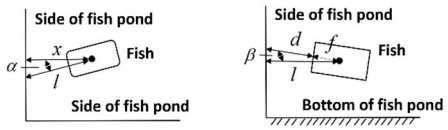

(a) (b)

Fig.3 Different perspectives of robotic fish in the fish pond.
(a) Top view. (b) Side view.

In Fig. 3, α is the yaw angle of the robotic fish, β is the pitch angle, f is the distance from the center point of robotic fish to the head boundary, d is the distance from the head of the fish to the pool's boundary, and l is the distance from the center point to the intersection line between the horizontal plane and the side of the pool. According to the angle relation, the abscissa x of the point can be calculated as (1):

$$x = (d + f)\cos\beta\cos\alpha \tag{1}$$

The above is the calculation process of the data obtained by the head sensor. Using the similar principle, the ordinate y of this point can be obtained through the left and right sensors.

Ideally, the faces of three sensors are different, then two opposite sensors are together used to calculate the coordinate of the direction and the other one is used to determine the coordinate in the other direction. When two of sensors face the same in the motion of fish, then the mean value is taken as the final coordinate in corresponding direction.

B. Medium-distance positioning

For the medium-distance range (within about 3 meters), this article uses BLE beacons and four signal receiving nodes to build a positioning system. After the real-time signal is transmitted to the network server, the approximate coordinates of the robotic fish are obtained through the four-point positioning method, and then the final coordinates are corrected by the K-Means-based clustering-grid supervision (CGS) algorithm proposed, so that the robotic fish positioning with a decimeter-level error is realized.

1) Signal conversion

This paper finally adopts a Beacon device that supports BLE5.0 low-power protocol as the signal base station. It is deployed on the robotic fish, and four receiving nodes that also support BLE5.0 are arranged in different locations on the site to obtain the signals sent by the BLE Beacon. The relationship between the transmit power and the received power of the signal can be expressed as follows [10]:

$$r_c = 100\times 10^{\frac{P_t - P_r}{10n}} = 10^{\frac{P_t - P_r}{10n}+2} \tag{2}$$

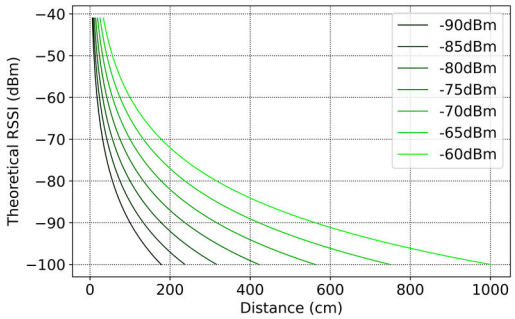

Fig.4 The relationship curve between signal strength and distance under different transmit power

In (2), r_c is the distance between the sending end and the receiving end (cm). P_t is the transmit power (dBm), P_r is the received power (dBm). Select six different levels of transmit power, then measure the signal strength at a distance of 1m from the transmitting base station under different levels of transmit power in the actual experimental environment, and calculate the value of environmental attenuation factor $n \approx 4.3$ according to (2). Substituting it and different transmit power values into (2), the theoretical signal strength varies with distance as shown in Fig. 4.

It is not difficult to see from Fig. 4 that the signal of the base station depletes rapidly in a close range, and as the distance increases, the signal attenuation becomes less noticeable. According to the theoretical curve, combined with the actual field requirements, it shows that in the range of 300cm, the discrimination is always good when the transmit power is -80dBm in Fig. 5(a). Fig. 5(b) shows the signal strength curve when the transmit power is -80dBm.

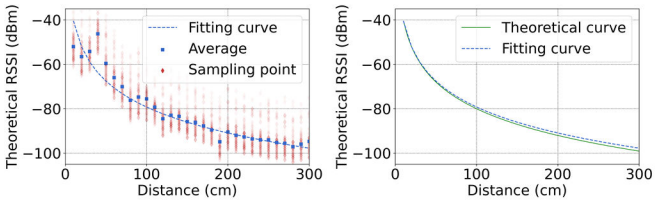

(a) (b)

Fig.5 The relationship between signal strength and distance when the transmit power is -80dBm. (a) Sampling point and fitting result. (b) Comparison of fitting curve and theoretical curve

The signal strength fitting curve when the transmitting power is -80dBm is as (3):

$$\hat{r}_c = 10^{\frac{-79.23-P_r}{38.8}+2} \tag{3}$$

2) Four-point positioning

As shown in Fig. 6(a), in theory, if the distance between each node and the base station is measured and used as the radius to make a circle, then any three circles are taken, they must intersect at one point, and the intersection is the location of the base station carried by the robotic fish. In reality, the three circles are often as shown in Fig. 6(b), that is, two or three of the three circles intersect in an area that is not a point, or two or three of the circles do not intersect.

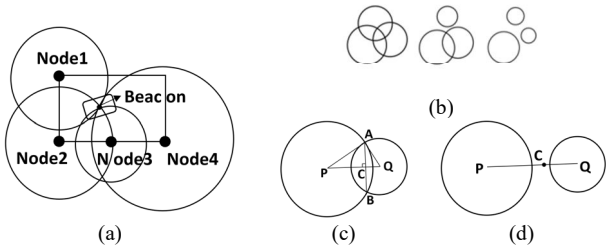

(a) (b) (c) (d)

Fig.6 Schematic diagram of four-point positioning method. (a) Ideal situation. (b) Realistic situation. (c) Two circles intersect. (d) Two circles do not intersect.

Assuming that two circles intersect at A and B, as shown in Fig. 6(c). PQ is known after arranging the position of the receiving node, and PA and AQ can be obtained according to the Euclidean formula. According to the Pythagorean theorem, PC can be obtained, and the coordinates of point C can be estimated according to (4). ζ is the abscissa or ordinate of the point.

$$\zeta_C = \zeta_P + \frac{(\zeta_Q - \zeta_P)PC}{PQ} \tag{4}$$

Assuming that the two circles don't intersect, as shown in Fig. 6(d). the coordinates of C can also be obtained according to the ratio of the radius of the two circles by replacing PQ with the sum of the radii of the two circles, and at the same time replace PC with the radius of circle P.

According to this method, this paper uses the average of the calculation results of a variety of different node combinations to estimate the coordinates of the robotic fish.

3) Clustering-grid Supervision (CGS)

In order to better correct the results of four-point positioning, this paper proposes a clustering-grid supervision (CGS) method based on K-Means[11]. As shown in Fig. 7, the pool is divided into 56 grids according to a fixed area.

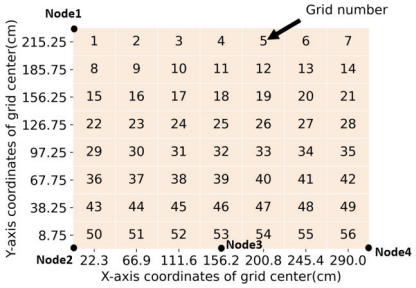

Fig.7 Meshing of the pool in the medium-distance range experiment

First, get the training set, that is, all the signal strength vectors sampled in each grid. The combination $x_i = (x_{r_1}, x_{r_2}, x_{r_3}, x_{r_4})$ in a group of the same grid received at the same time is a set of vectors, with a total of 11,200 records, and each record is marked with its grid number. Taking Node 3 as an example, a box plot of signal strength can be drawn as shown in Fig. 8. The perception of the signals sent from different grids by the four nodes is shown in Fig. 9.

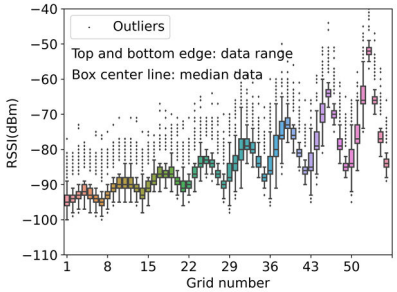

Fig. 8 The signal strength changes of Node 3

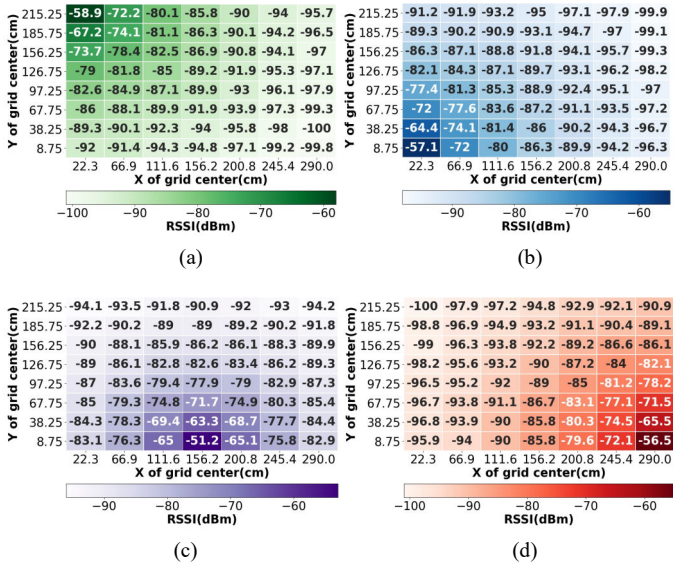

Fig. 9 Nodes' perception of the signal sent from different grids.
(a)Node 1. (b)Node 2. (c) Node 3. (d)Node 4.

After obtaining the training set data, execute the algorithm according to the following flow:

Algorithm 1 Clustering-grid supervision method

Input: $D=\{x_1,x_2,...,x_m\}$, training set; x_τ, the signal vector to be predicted; $k_{\max}$, the maximum amount of clusters

Output: λ_τ, the number of the grid to which x_τ belongs

1. **for** k=1,…, $k_{\max}$ **do**
2. Initialize the division of the cluster, $C_t=\varnothing(t=1,2,...,k)$
3. Choose k samples as the initial k centroid vectors $\{\mu_1,...,\mu_k\}$
4: **do**
5: for $i=1,...,k$, Calculate the distance: $d_{ij}=\left|x_i-\mu_j\right|^2$
6: Label x_i with the grid λ_i corresponding to the smallest d_{ij}. Now update $C_{\lambda_i}=C_{\lambda_i}\cup\{x_i\}$
7: for $j=1,2,...,k$, recalculate the centroid vector for all sample points in C_j: $\mu_j=\left|C_j\right|^{-1}\sum_{x\in C_j}x$
8: **while** None of the centroid vectors have changed
9: **end while**
10: Calculate clustering error: $E=\sum_{i=1}^{k}\sum_{x\in C_i}\left|x-\mu_i\right|^2$
11: Save the cluster number k and the corresponding clustering division result C and the error E
12: **end for**
13: Select k_{best} according to elbow method [11]
13: Substitute x_τ into the clustering division corresponding to k_{best} to predict the grid number λ_τ it belongs to

This paper selects the number of clusters k=16, as shown in Fig. 10(a), by comparing the actual grid label with the predicted results, it can be seen that the probability of the algorithm prediction results falling into the correct grid clustering or its neighborhood is 85%.

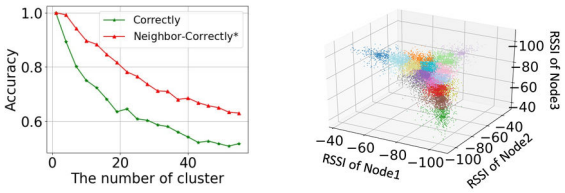

Fig. 10 Grid clustering results.
(a) Accuracy when different clustering numbers are taken. (b) Clustering effect chart drawn according to the three nodes.

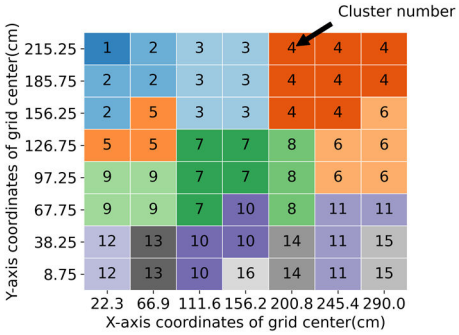

Fig. 11 The final clustering result of pool grid

In order to intuitively see the clustering effect, the signal strength obtained by three nodes is selected to draw the clustering distribution effect diagram, as shown in Fig. 10(b). It can also be seen that when k =16, the clustering effect is significant. The 56 grid numbers were mapped to the 16 cluster numbers after clustering, as shown in Fig. 11.

4) Coordinate calculation of robotic fish

The grid of robotic fish is predicted according to the above method, and a random coordinate is generated in the clustering area. The coordinate is weighted with the result calculated by the four-point positioning method according to (5):

$$\zeta=\alpha\zeta_m+(1-\alpha)\zeta_t \tag{5}$$

α is the supervision factor, which can be adjusted according to the environment. ζ is the coordinate of the fish finally given; ζ_m is randomly generated coordinate in the predicted grid; ζ_t is the coordinate calculated according to the four-point positioning method. Since ζ_m is randomly generated coordinate, the direct calculation of (5) will lead to great fluctuation of the final trajectory, while the four-point positioning method can better reflect the overall motion direction. Therefore, the difference between the current coordinate ζ_i and the coordinate of the previous sampling time ζ_{i-1} should be made to obtain $\Delta\zeta$, and similarly, $\Delta\zeta_t$ should be obtained. By comparing the symbols of $\Delta\zeta$ and $\Delta\zeta_t$, if the symbols are same, the current corresponding direction coordinate shall be retained; otherwise, the direction coordinate of the previous time shall still be used to ensure that the

correctness of the overall movement trend shall be taken into account while reducing the positioning error.

IV Experimental Results and Analysis

In order to verify the positioning effect of the proposed method, more than 30 groups of experiments were conducted in the short-distance range and nearly 60 groups of experiments were conducted in the medium-distance range. The experiment covered a variety of different movements of robotic fish. Some of the experimental results and analysis are shown as follows:

A. Short-distance positioning

1) Orientation recognition

According to the orientation recognition process in Chapter 3 of, the initial direction can be determined as shown in Fig. 12.

Fig. 12 The result of orientation recognition

2) Calculation of trajectories

The size of the pool is 72*52cm, and the speed of the fish is about 0.25~0.4BL/s. Fig. 13 shows three of experiments. The average movement distance of the fish in each group is 30cm, and the average number of samples in each group is 32.

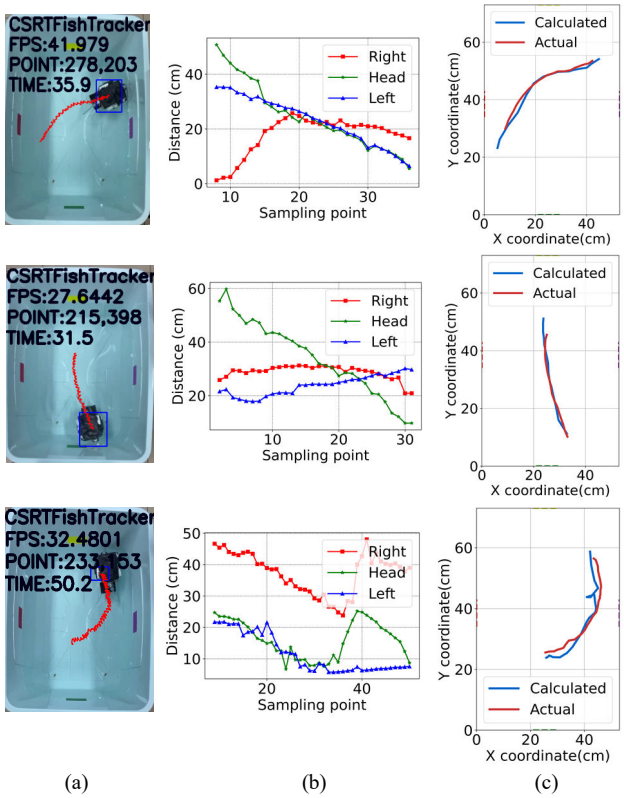

(a) (b) (c)

Fig. 13 Results of three groups of short-distance experiments. (a) Coordinate calculated by sensors. (b) Actual fish trajectories obtained by camera. (c) Comparison between calculated and actual trajectories.

B. Medium-distance positioning

In the medium-distance experiment, the size of the pond is 300cm*235cm. As shown in Fig. 7, there are four nodes used to receive signals from the beacon, and the plane where the nodes are located is 20cm from the surface of the water. Set the coordinate system with the lower left corner as the origin, where the coordinate of Node1 is (0,230), the coordinate of Node2 is (0,0), the coordinate of Node3 is (156,0), and the coordinate of Node4 is (290,0); The average duration of each of the following experiments is 8 minutes, and more than 20,000 pieces of data can be collected on average in each experiment. Here are three groups of results. Fig. 14 shows the original signals and filtering values of the first group of experiments. Fig. 15 shows the positioning results.

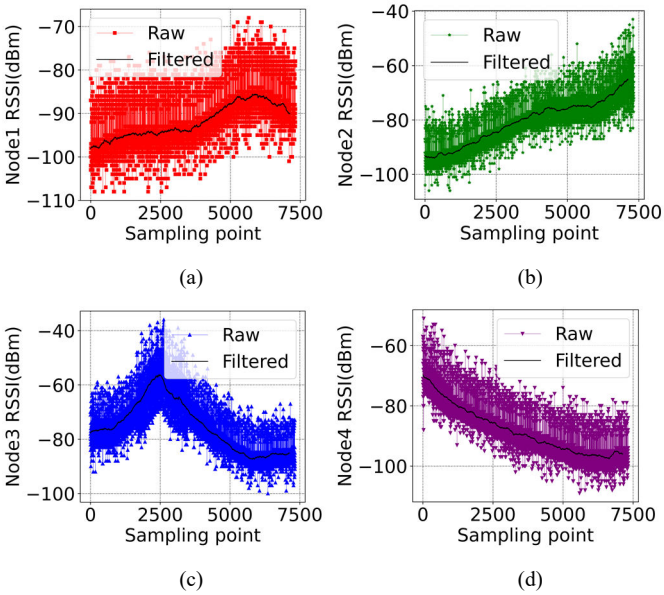

(a) (b) (c) (d)

Fig. 14 Signal values of the first group in the following experiments. (a) Node 1. (b) Node 2. (c) Node 3. (d) Node 4.

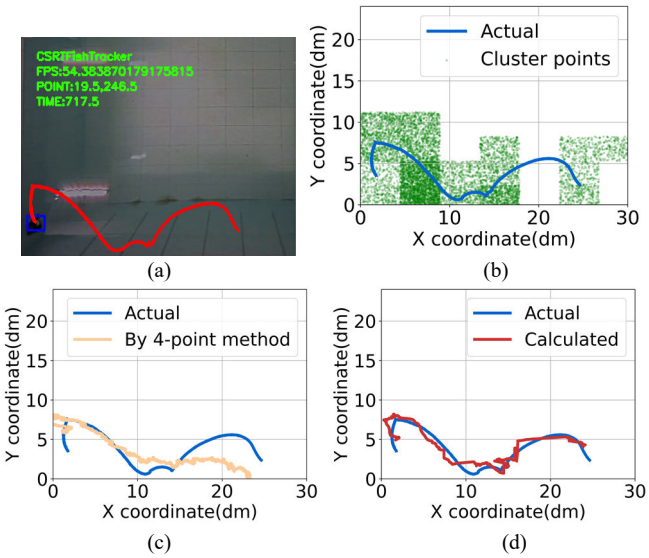

(a) (b) (c) (d)

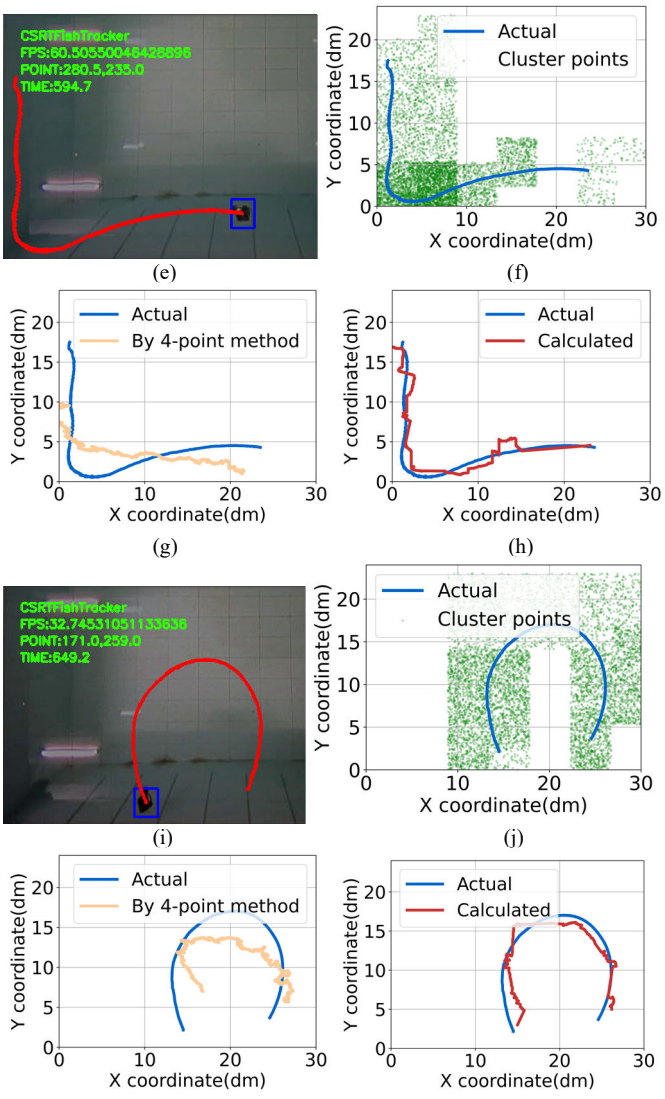

Fig. 15 Results of three groups of medium-distance experiments. (a,e,i) Actual trajectories obtained by camera. (b,f,j) Random point distribution generated during the grid supervision. (c,g,k) Trajectories preliminarily calculated by four-point positioning method. (d,h,l) Comparison between calculated and actual trajectories.

C. Evaluation

Fig. 16 respectively shows the positioning error statistics of all the experiments in short and medium distances.

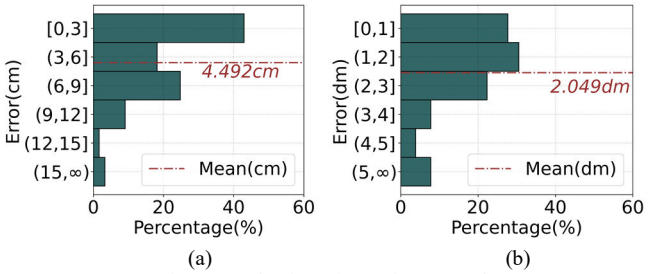

Fig. 16 Evaluation of experiment results. (a) Distribution and mean value of positioning error in short range. (b) Distribution and mean value of positioning error in medium range.

It is not difficult to see from Fig. 16(a) that in short range, positioning errors are mostly concentrated within the range of 0~6.0cm, and no error more than 12.0cm. The average error is 4.492cm, and the coordinate error within 3.0cm accounted for 42.98%. As can be seen from Fig. 16(b), although the error distribution tends to be discrete, about 60% of coordinate errors are in the range of 0~ 2.0dm, and the mean error is 2.049dm.

V Conclusion

In this paper, a combined indoor robotic fish positioning method is proposed, which provides a new idea for the position observation of robotic fish in the research work in the experimental environment. In future, we will consider introducing the motion state model of robotic fish and using the lateral array sensor to further improve the positioning accuracy.

Acknowledgment

This work was supported by National Nature Science Foundation of China (62033013, 61903362, 62003341, 61973303).

References

[1] J. J. Leonard, and H. F. Durrant-Whyte, “Mobile robot localization by tracking geometric beacons,” IEEE Transactions on Robotics and Automation, vol. 7, no. 3, pp. 376-382, 1991.

[2] D. Isla, “RoboTuna project to model real fish,” The Tech Magazine, vol. 115, no. 49, pp. 13, 1995.

[3] T. Li, G. Li, Y. Liang, T. Cheng, J. Dai, X. Yang, B. Liu, Z. Zeng, Z. Huang, and Y. Luo, “Fast-moving soft electronic fish,” Science Advances, vol. 3, no. 4, pp. e1602045, 2017.

[4] J. Zhu, C. White, D. K. Wainwright, V. D. Santo, and H. Bart-Smith, “Tuna robotics: A high-frequency experimental platform exploring the performance space of swimming fishes,” Science Robotics, vol. 4, no. 34, pp. eaax4615, 2019.

[5] M. Mohanakrishnan, and P. A. Iyamperumal, “Development of Subcarangiform Bionic Robotic Fish Propelled by Shape Memory Alloy Actuators,” Defence Science Journal, vol. 71, no. 1, pp. 94-101, 2021.

[6] W. Wang, and G. Xie, “Online High-Precision Probabilistic Localization of Robotic Fish Using Visual and Inertial Cues,” IEEE Transactions on Industrial Electronics, vol. 62, no. 2, pp. 1113-1124, 2015.

[7] Novak, P. Cisar, M. Bruneau, P. Lotton, and L. Simon, “Localization of sound-producing fish in a water-filled tank,” The Journal of the Acoustical Society of America, vol. 146, no. 6, pp. 4842-4850, 2019.

[8] X. Zheng, W. Wang, M. Xiong, and G. Xie, “Online State Estimation of a Fin-Actuated Underwater Robot Using Artificial Lateral Line System,” IEEE Transactions on Robotics, vol. 36, no. 2, pp. 472-487, 2020.

[9] Y. Aimin, L. Shanshan, L. Honglei, and J. Donghao, “Edge extraction of mineralogical phase based on fractal theory,” Chaos, Solitons & Fractals, vol. 117, pp. 215-221, 2018.

[10] P. Wang, and Y. Luo, "Research on Indoor Location Algorithm Based on RSSI Ranging.", vol.1, pp. 1694-1698, 2017.

[11] G. Wu, J.-l. Zhang, and D. Yuan, “Automatically Obtaining K Value Based on K-means Elbow Method,” Comput. Eng. Softw, vol. 40, pp. 167-170, 2019.